

Uncertainty Quantification of Radio Wave Propagation over Irregular Terrains Using Adaptive Polynomial Chaos Expansion

Sicheng An, Luca Di Rienzo, *Senior Member, IEEE*, Hao Qin, *Member, IEEE*, Xingqi Zhang, *Senior Member, IEEE* Lorenzo Codecasa, *Member, IEEE*

Abstract—Accurate modeling of radio wave propagation over irregular terrains is crucial for designing reliable wireless communication systems in such environments, yet uncertainties in the antenna configuration are not quantified within deterministic models. In this paper, we present, to the best of our knowledge, the first uncertainty quantification (UQ) study of realistic antenna configurations for irregular-terrain propagation. An adaptive polynomial chaos expansion (APCE) method is improved and coupled with a two-way parabolic wave equation (PWE) method to address this problem efficiently. The polynomial basis is extended according to variance contributions and terminated by a composite criterion combining validation error and sample-to-basis ratio, enabling stable coefficient estimations via least-square regression without additional regularization. Convergence analysis shows a monotonic error decay with increasing training samples, producing compact, low-interaction models and improved accuracy and robustness over the previous APCE methods. For two realistic terrain profiles, the proposed method accurately predicts the mean and the 5th-95th percentile range of the path loss, matching Monte Carlo (MC) references using only 30 PWE simulations. Using a fixed sampling budget (e.g., $N_s = 30$), APCE outperforms standard and sparse PCE, with the largest gains observed for the 5th and 95th percentile estimates; as the sample size increases, APCE maintains low errors with reduced trial-to-trial variability.

Index Terms—Antenna uncertainty, adaptive polynomial chaos expansion, irregular terrains, parabolic wave equation method, radio wave propagation, uncertainty quantification.

I. INTRODUCTION

ACCURATE modeling of radio wave propagation over irregular terrains is crucial to developing and optimizing reliable wireless communication systems in such scenarios [1]–[3]. A variety of numerical techniques, including finite difference time domain (FDTD) methods [4], integral equation-based methods [5], and parabolic wave equation (PWE) methods [6], have been developed to handle these scenarios. Among these approaches, the two-way PWE method has emerged

as an accurate and computationally efficient approach for modeling radio wave propagation in such environments [7]–[9]. However, accurate numerical simulation requires precise information about antenna configuration parameters, which are often subject to significant uncertainties in practical deployments [10], [11].

To analyze the impact of uncertain parameters in computational electromagnetics problems, various uncertainty quantification (UQ) techniques have been applied, e.g. [12], [13]. The Monte Carlo (MC) method is widely used due to its straightforward implementation and high reliability, but it typically demands a large number of simulations because of its slow convergence. To address this limitation, polynomial chaos expansion (PCE) methods have been introduced as more efficient alternatives [14], [15]. More recently, sparse regression techniques have been incorporated into PCE to enhance computational efficiency and robustness to noisy data [16], [17]. Nevertheless, PCE representations of realistic models are not always exactly sparse, so the sparsity assumption only holds approximately. As a consequence, for both classical PCE and sparse PCE, the selection of an appropriate polynomial basis remains a difficult and crucial task [18], [19]. Some adaptive PCE (APCE) approaches have been proposed, but they still build on this sparsity assumption [19], [20].

Although recent works have combined PWE methods with different UQ approaches to quantify the uncertainty of wave propagation in tunnel environments [21], [22], three key challenges remain insufficiently addressed in the context of radio wave propagation over irregular terrains. First, uncertainties in the antenna configuration are often not treated, which may lead to propagation predictions that are overly optimistic and insufficiently robust with respect to realistic installation tolerances. Second, when constructing a surrogate model using PCE, the expansion must be truncated to a finite basis; an inappropriate choice of polynomial terms may lead to poor approximation accuracy or high computational cost. Third, the sparsity assumption on the expansion coefficients does not hold universally across all applications.

In this paper, we present, to the best of our knowledge, the first UQ study of realistic antenna configuration uncertainties for irregular-terrain propagation. Building on the anisotropic basis extension strategy in [23], we propose an adaptive polynomial chaos expansion (APCE) method with a composite heuristic stopping criterion designed for fixed and limited sampling budgets. The proposed method is evaluated

Sicheng An, Luca Di Rienzo, and Lorenzo Codecasa are with the Dipartimento di Elettronica, Informazione e Bioingegneria, Politecnico di Milano, Milan 20133, Italy (e-mail: sicheng.an@polimi.it; luca.dirienzo@polimi.it; lorenzo.codecasa@polimi.it).

Hao Qin is with the School of Electronics and Information Engineering, Sichuan University, Chengdu 610065, China (e-mail: hao.qin@scu.edu.cn).

Xingqi Zhang is with the Department of Electrical and Computer Engineering, University of Alberta, Edmonton, AB T6G 2H5, Canada (e-mail: xingqi.zhang@ualberta.ca).

Color versions of one or more of the figures in this paper are available online at <http://ieeexplore.ieee.org>.

Digital Object Identifier: XXXX

on two realistic terrain profiles. Convergence analysis shows a monotonic reduction of the leave-one-out validation error as the sampling budget increases, and improved accuracy and robustness compared with [23]. In addition, the mean, 5th percentile, and 95th percentile estimation of the APCE are consistent with the MC reference. Under the same sampling budget, the proposed method yields smaller and more stable errors than both standard and sparse PCEs, particularly for percentile estimates.

The remainder of the article is organized as follows. Section II introduces the deterministic modeling method we used. Section III presents the proposed APCE approach. Section IV reports numerical results on two realistic terrain profiles, including convergence analysis and uncertainty quantification. Finally, Section V summarizes the main findings and concludes the paper.

II. DETERMINISTIC MODELING

The PWE method follows from the Helmholtz equation for free space:

$$\left(\frac{\partial^2}{\partial x^2} + \frac{\partial^2}{\partial y^2} + \frac{\partial^2}{\partial z^2} + k_0^2 \right) \varphi(x, y, z) = 0, \quad (1)$$

where k_0 is the free-space wavenumber and x , y , and z stand for the Cartesian coordinates. Moreover, $\varphi(x, y, z)$ denotes a scalar electric or magnetic potential. Assuming the wave propagation is predominant along the z -axis, a solution to (1) can be cast as

$$\varphi(x, y, z) = u(x, y, z)e^{-jk_0z}, \quad (2)$$

where u is the reduced plane wave solution. Substituting (2) into (1) and assuming [25]

$$\left| \frac{\partial u^2}{\partial z^2} \right| \ll k_0 \left| \frac{\partial u}{\partial z} \right|, \quad (3)$$

the standard PWE reads [25]:

$$\frac{\partial u}{\partial z} = \frac{1}{2jk_0} \left(\frac{\partial^2}{\partial x^2} + \frac{\partial^2}{\partial y^2} \right) u. \quad (4)$$

After using a split-step Fourier transform technique, the field distribution in each cross-section is updated from the field in the previous cross-section by [7]

$$\hat{u}(k_x, k_y, z) = \mathcal{F}\{u(x, y, z); x, y\}, \quad (5)$$

$$u(x, y, z + \Delta z) = \mathcal{F}^{-1} \left\{ \exp\left(-\frac{j(k_x^2)\Delta z}{2k_0}\right) \exp\left(-\frac{j(k_y^2)\Delta z}{2k_0}\right) \hat{u}(k_x, k_y, z); k_x, k_y \right\}, \quad (6)$$

where \mathcal{F} and \mathcal{F}^{-1} denote the Fourier transform pairs, k_x and k_y are spectral variables. When the wave reaches an obstacle, it is decomposed into forward and backward propagating components, as shown in Fig. 1. The forward propagating wave is predicted by (6), and the backward propagating wave is updated by

$$u(x, y, z - \Delta z) = \mathcal{F}^{-1} \left\{ \exp\left(\frac{j(k_x^2)\Delta z}{2k_0}\right) \exp\left(\frac{j(k_y^2)\Delta z}{2k_0}\right) \hat{u}(k_x, k_y, z); k_x, k_y \right\}, \quad (7)$$

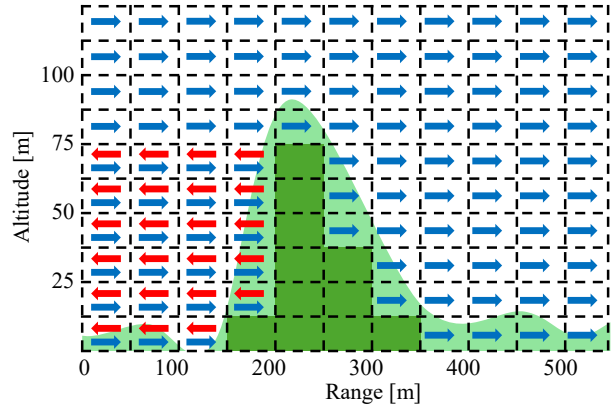


Fig. 1. Two-way PWE method over an irregular terrain. The forward (blue) and backward (red) propagating waves are shown; the light-green domain represents the true terrain profile, and the dark-green denotes its discretized approximation. For clarity, the discretization grid is exaggerated in this illustration; in the actual simulations, a much finer terrain discretization is employed.

III. ADAPTIVE POLYNOMIAL CHAOS EXPANSION

A. Overview

Polynomial chaos expansion provides a surrogate model for the dependence between a random N_d -dimensional input random vector ξ and a quantity of interest (QoI) $q(\xi)$ by expanding QoI onto an orthonormal polynomial basis [15]:

$$q(\xi) \approx \sum_{\alpha \in \mathcal{A}} u_\alpha \psi_\alpha(\xi), \quad (8)$$

where $\psi_\alpha(\xi)$ is the multivariate polynomial orthonormal with respect to the joint probabilistic distribution of the input variables. To obtain a finite representation, the polynomial basis set \mathcal{A} is usually truncated using a maximum total-order O_T criterion, as shown in Appendix A. However, it is easy to see in Table A-I that the number of polynomial basis functions increases dramatically with the increase of the maximum total order. To address this issue, several truncation strategies have been proposed, such as the hyperbolic truncation scheme [17] and the maximum interaction order truncation [26]. Although these schemes effectively suppress high-order interaction terms, selecting appropriate hyperparameters for each method remains challenging.

To overcome these limitations and fully utilize the potential of available samples, an APCE framework [18] is adopted here, where a specific basis extension strategy is coupled with well-designed termination criteria. The main steps are summarized as follows:

- **Polynomial family selection:** identify the orthonormal polynomial families associated with the input distributions, according to [27].
- **Sample set generation:** generate realizations of the uncertain input variables and calculate the corresponding QoIs by Latin Hypercube Sampling (LHS) [28].
- **Basis extension:** expand the polynomial basis from the empty set using an adaptive basis-increment strategy (Sec. III-B).

- **Coefficient calculation and error evaluation:** compute PCE coefficients and assess the validation error. (Sec. III-C).
- **Termination criteria:** terminate when the established convergence criteria are fulfilled; otherwise, continue extension (Sec. III-D).

Compared with standard and sparse PCE formulations, as shown in Appendices A and B, the proposed adaptive scheme uses only the available samples to drive basis enrichment and does not require any user-defined parameters, which is particularly attractive when only a moderate number of training samples is affordable. Next, we will introduce the basis extension algorithm, coefficient calculation, error evaluation, and termination criterion in detail.

B. Basis Extension

Since the sparsity assumption is not always satisfied in practical PCE models, the basis extension method [23] is adopted, where two sets of multi-indices of polynomial terms are introduced:

- the candidate set \mathcal{A}_{cand} containing multi-indices that are eligible for further expansion;
- the old set \mathcal{A}_{old} , containing multi-indices that have already been used for the expansion.

The expansion condition is defined with respect to the old set \mathcal{A}_{old} only, as shown in Algorithm 1.

The multi-indices are extended according to the variance contribution. Suppose we have N_q QoIs $\{q_1, q_2, \dots, q_{N_q}\}$, each QoI q_i admits its own set of PCE coefficients. Let $u_{\alpha,i}$ denote the PCE coefficient associated with the basis function $\Psi_{\alpha}(\xi)$ for i -th QoI. To quantify the overall contribution of a multi-index α_k across all QoIs, we define

$$u_{\alpha_k}^{\nu} = \sum_{i=1}^{N_q} (u_{\alpha_k,i})^2 \quad (9)$$

which is proportional to the fraction of variance explained by the corresponding polynomial basis function Ψ_{α_k} over all QoIs. Collectively, the contribution of all polynomial terms form the vector $\mathbf{u}_{\alpha}^{\nu} = \{u_{\alpha_1}^{\nu}, \dots, u_{\alpha_{N_p}}^{\nu}\}$, where N_p is the total number of retained polynomial basis functions. Ranking the entries $u_{\alpha_k}^{\nu}$ provides a simple yet effective criterion to drive the basis-extension procedure toward polynomial directions that explain most of the total variance across all QoIs.

At each iteration, multi-indices adjacent to the index with the largest variance contribution are added to the basis. Furthermore, to avoid overfitting of the PCE model, we impose a maximum polynomial order and exclude any polynomial whose order exceeds this limit. The anisotropic basis-extension procedure is summarized in Algorithm 1.

C. Coefficient calculation and error evaluation

The PCE coefficients are determined using a regression-based approach [15]. Let $\{\xi^{(1)}, \dots, \xi^{(N_s)}\}$ be a sample set of the input parameters, and let $\mathbf{q} = (q^{(1)}, \dots, q^{(N_s)})^T$ be the corresponding vector of model response. Let us define the regression matrix Ψ with entries $\Psi_{ij} = \psi_j(\xi^{(i)})$. According

Algorithm 1 Anisotropic basis extension for APCE

- 1: **Input:** Contribution vector $\mathbf{u}_{\alpha}^{\nu}$, candidate set \mathcal{A}_{cand} , and old set \mathcal{A}_{old}
 - 2: **Output:** Set of multi-indices $\Delta\mathcal{A}$, and updated \mathcal{A}_{cand} and \mathcal{A}_{old}
 - 3: $\alpha_{k'} = \arg \max_{\alpha_k \in \mathcal{S}_{cand}} \|\mathbf{u}_{\alpha}^{\nu}\|$;
 - 4: $\mathcal{A}_{cand} = \mathcal{A}_{cand} \setminus \{\alpha_{k'}\}$;
 - 5: $\mathcal{A}_{old} = \mathcal{A}_{old} \cup \{\alpha_{k'}\}$;
 - 6: $\Delta\mathcal{A} = \emptyset$;
 - 7: **for** i in $1, \dots, d$ **do**
 - 8: $\beta_i = \alpha_{k'} + e_i$;
 - 9: **if** $\beta_i - e_j \in \mathcal{A}_{old} \forall j = 1, \dots, d$ **then**
 - 10: $\Delta\mathcal{A} = \Delta\mathcal{A} \cup \{\beta_i\}$;
 - 11: **end if**
 - 12: **end for**
 - 13: $\mathcal{A}_{cand} = \mathcal{A}_{cand} \cup \Delta\mathcal{A}$;
-

to (8), the coefficients \mathbf{u} can be calculated by least squares regression:

$$\hat{\mathbf{u}} = \arg \min \|\Psi\mathbf{u} - \mathbf{q}\|_2^2 \quad (10)$$

Owing to the revised basis-extension algorithm, the resulting PCE basis is sufficiently compact that no additional ℓ_1 - or ℓ_2 -type regularization is required in the coefficient estimation step. Therefore, the PCE coefficients are calculated directly from ordinary least squares regression (10), whose closed-form solution is given by the Moore-Penrose pseudoinverse:

$$\hat{\mathbf{u}} = (\Psi^T \Psi)^{-1} \Psi^T \mathbf{q} \quad (11)$$

The validation error at each iteration is evaluated using the relative ℓ_2 error:

$$\varepsilon_v = \frac{\|q(\xi_v) - \sum_{\alpha \in \mathcal{A}} u_{\alpha} \Psi_{\alpha}(\xi_v)\|_2}{\|q(\xi_v)\|_2} \quad (12)$$

where ξ_v denote the validated samples. In practice, the leave-one-out cross-validation (LOOCV) error is used; each surrogate model is constructed with one sample removed from the training set and then evaluated on the excluded sample. For multi-output QoIs, the overall validation error is obtained by averaging the relative errors over all output components.

D. Termination Criteria

A suitable stopping criterion is essential for achieving good approximation performance. In contrast to traditional approaches that rely on hard thresholds on properties of the regression matrix [29], [30] or on the approximated error [23], [31], we proposed a composite heuristic termination criterion:

- the number of polynomial terms is required to exceed 0.25 times the number of available samples, to avoid premature termination.
- to ensure the accuracy and stability of the regression, the algorithm is forced to terminate once the number of polynomial terms exceeds 0.5 times the number of samples;
- if the minimum LOOCV ε_v does not decrease for consecutive iterations, the algorithm terminates early to avoid overfitting;

- if the validation error reaches the prescribed target threshold, the algorithm terminates.

The lower and upper bounds of the polynomial terms is motivated by the empirical rule of thumb that, when the number of samples is about four times the number of unknown coefficients, the ordinary least-squares estimate in (11) is already sufficiently accurate; and that accurate and stable ordinary least-squares regression typically requires at least twice as many samples as polynomial coefficients [16].

IV. EXAMPLES IN REALISTIC IRREGULAR TERRAINS

A. Overview

We validate the proposed framework over two realistic terrain profiles in northern Denmark, namely Jerslev and Hjørringvej [32], shown in Fig. 2. In all cases, the ground is modeled as a lossy dielectric with relative permittivity $\epsilon_r = 4.5$ and loss tangent $\tan \delta = 0.07$. For the two-way PWE simulations, the spatial steps are set to $\Delta x = 50$ m and $\Delta y = 0.5$ m, based on [33]. A unit-amplitude Gaussian source is used, and the total propagation distances are 5 km and 10 km for the Jerslev and Hjørringvej profiles, respectively.

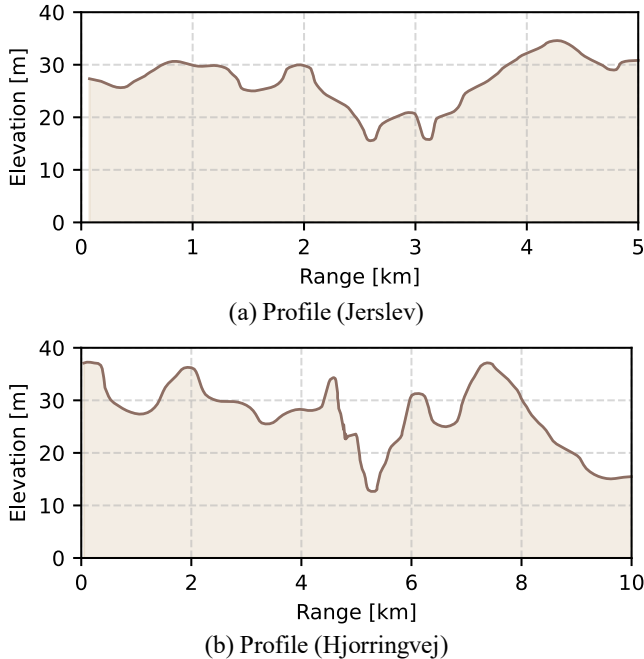


Fig. 2. Jerslev and Hjørringvej terrain profiles used to validate the proposed uncertainty quantification framework.

We consider the uncertainties from two sources. The first group consists of geometric parameters, including transmitter height, elevation angle, and receiver height, as illustrated in Fig. 3. The second group includes internal transmitter parameters, such as the operating frequency and the antenna beamwidth. All uncertain parameters are modeled as Beta random variables with shape parameters (3, 3) and bounded support, as summarized in Table I. This choice yields a Gaussian-like distribution while enforcing strict physical bounds on

each parameter, which is particularly appropriate for modeling installation tolerances and equipment variations that cannot exceed prescribed limits [23], [34].

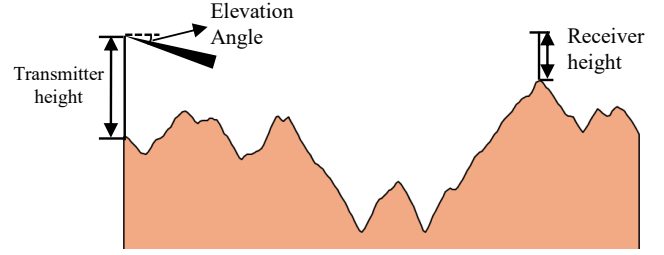


Fig. 3. Geometry of the antenna configuration and definition of the uncertain geometric parameters: transmitter height, elevation angle, and receiver height.

TABLE I
UNCERTAIN ANTENNA CONFIGURATION PARAMETERS AND THEIR BOUNDS. THEIR PROBABILITY Beta(3, 3) DENOTES A BETA DISTRIBUTION WITH SHAPE PARAMETERS 3 AND 3

Parameter	Unit	Distribution	Interval	Reference
Transmitter height	m	Beta(3, 3)	[9, 13]	[32]
Receiver height	m	Beta(3, 3)	[1, 4]	[32]
Elevation angle	°	Beta(3, 3)	[-3, 3]	[10], [11]
Beamwidth	°	Beta(3, 3)	[4, 12]	[10], [11]
Frequency MHz		Beta(3, 3)	[410, 460] (Jerslev) [920, 1020] (Hjørringvej)	[10], [11], [32]

The QoIs is the path loss along the propagation range, derived from the received power at the specified received height. Let r_i , $i = 1, \dots, N_r$, denote the equidistance locations, and let $q_i = q(r_i)$ be the corresponding random path-loss value at range r_i . Collecting these into a vector, we define $\mathbf{q} = [q_1, \dots, q_{N_r}]^T$. From the PCE surrogate model, we estimate at each spatial location the mean $\mathbb{E}(pl_i)$, the 5th percentile $\mathbb{Q}^5(q_i)$, and the 95th percentile $\mathbb{Q}^{95}(q_i)$, which we assemble into the vectors $\mathbb{E}(\mathbf{q})$, $\mathbb{Q}^5(\mathbf{q})$, and $\mathbb{Q}^{95}(\mathbf{q})$, respectively. The mean characterizes the expected propagation behavior, while the 5th and 95th percentiles define a 90% reliability interval along the propagation range. To assess the accuracy of various methods, the relative errors on the mean, 5th percentile, and 95th percentile are defined as:

$$e_r(\mathbb{E}(\mathbf{q})) := \frac{\sqrt{\sum_{i=1}^{N_r} [\mathbb{E}(q_i) - \mathbb{E}_{ref}(q_i)]^2}}{\sqrt{\sum_{i=1}^{N_r} [\mathbb{E}_{ref}(q_i)]^2}}, \quad (13)$$

$$e_r(\mathbb{Q}^5(\mathbf{q})) := \frac{\sqrt{\sum_{i=1}^{N_r} [\mathbb{Q}^5(q_i) - \mathbb{Q}_{ref}^5(q_i)]^2}}{\sqrt{\sum_{i=1}^{N_r} [\mathbb{Q}_{ref}^5(q_i)]^2}} \quad (14)$$

$$e_r(\mathbb{Q}^{95}(\mathbf{q})) := \frac{\sqrt{\sum_{i=1}^{N_r} [\mathbb{Q}^{95}(q_i) - \mathbb{Q}_{ref}^{95}(q_i)]^2}}{\sqrt{\sum_{i=1}^{N_r} [\mathbb{Q}_{ref}^{95}(q_i)]^2}} \quad (15)$$

where $\mathbb{E}(\cdot)$, $\mathbb{Q}^5(\cdot)$, and $\mathbb{Q}^{95}(\cdot)$ are the mean, 5-th percentile, and 95-th estimator, whereas $\mathbb{E}_{ref}(\cdot)$, $\mathbb{Q}_{ref}^5(\cdot)$, and $\mathbb{Q}_{ref}^{95}(\cdot)$ are the reference estimators computed from 10^5 MC simulations. The details about these estimators are shown in Appendix C.

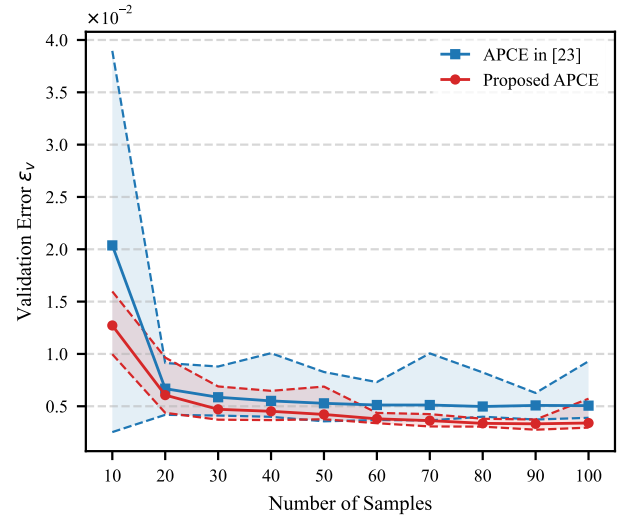
B. Convergence Analysis

The proposed APCE method automatically selects the polynomial basis functions used in the PCE model. Before estimating the path-loss statistics, we first investigate the convergence behavior of the APCE with respect to the number of training samples. To this end, we analyze the validation error, as defined in (12), for different sample sizes. Ten sampling levels are considered, $N_s = 10, 20, 30, 40, 50, 60, 70, 80, 90, 100$. For each N_s , thirty independent training sets are generated, and corresponding PCE models are constructed. We further benchmark our approach against the APCE method of [23], which employs the same basis-extension algorithm. The resulting distributions of the validation error are summarized in Fig. 4.

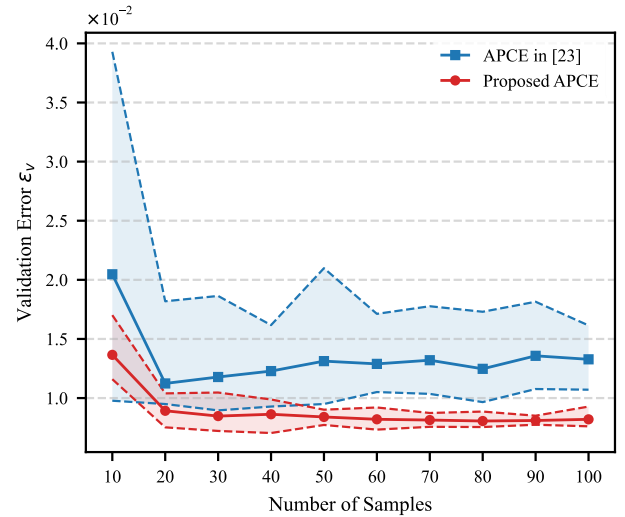
As shown in Fig. 4, the validation error decreases monotonically for both terrain profiles, with a pronounced reduction when N_s increases from 10 to about 30. For larger sample sizes, the error curves gradually flatten, and the variability across the thirty realizations becomes small, indicating that the surrogate model has essentially converged and that the adaptive basis-selection procedure is stable. Fig. 4 also highlights a consistent advantage of the proposed method over the APCE in [23]. For most sampling levels, the proposed APCE attains a lower validation error. Moreover, the minimum-maximum ranges and whiskers of the proposed method are generally narrower, demonstrating reduced dispersion across independent realizations and thus a more stable and reliable performance. This behavior indicates that the proposed APCE more effectively controls unnecessary basis growth and mitigates sensitivity to the particular training set, resulting in improved generalization.

To further analyze the adaptivity of the proposed APCE, we report in Tables II and III the number of selected polynomials, the maximum polynomial order, and the maximum interaction order of the polynomial bases constructed by the proposed APCE method. The maximum polynomial order is defined as the highest order of any individual polynomial basis function, whereas the maximum interaction order is defined as the largest number of distinct variables involved in a single multivariate basis term. In all cases, the polynomial order is limited to at most five. From Tables II and III, it can be observed that the proposed method automatically adjusts the number of selected basis functions as the sample size increases, while effectively suppressing high-order interaction terms. In particular, already at $N_s \approx 30$ the selected bases remain compact and are dominated by low interaction orders (predominantly two), with higher-order interactions appearing only sporadically as N_s becomes larger. This behavior suggests that the dominant contributions to the response can be captured using relatively low-order and low-interaction polynomials, which improves robustness and reduces the risk of overfitting.

In this convergence study, we deliberately set a very strict target error of 10^{-3} , which is not reached in the plotted



(a) Validation error ε_v (Jerslev)



(b) Validation error ε_v (Hjorringvej)

Fig. 4. Validation error ε_v [defined in (12)] of the path-loss surrogate versus the number of training samples N_s for the Jerslev and Hjorringvej terrain profiles. The solid lines represent the mean validation error, while the shaded bands (bounded by dashed lines) indicate the minimum and maximum errors across the independent trials.

curves in Fig. 4. This is by design: once the error stops decreasing significantly, the composite heuristic termination criterion triggers an early stop, so that basis enrichment is halted automatically before the prescribed target error is attained, thereby avoiding overfitting and unnecessary growth of the polynomial basis. Since both the validation error and the basis statistics exhibit diminishing returns beyond $N_s \approx 30$, we adopt $N_s = 30$ as a cost-effective sampling budget in the subsequent UQ study and use larger N_s only for additional robustness comparisons.

C. Uncertainty Quantification

With $N_s = 30$ samples, we construct a surrogate model using the proposed APCE method. Fig. 5 shows the mean path

TABLE II

NUMBER OF BASIS FUNCTIONS, MAXIMUM POLYNOMIAL ORDER, AND MAXIMUM INTERACTION ORDER SELECTED UNDER DIFFERENT SAMPLE SIZES (JERSLEV). POLYNOMIAL ORDER AND INTERACTION ORDER OF 0 INDICATES THAT ONLY THE CONSTANT TERM IS SELECTED.

Number of Samples	Number of Basis Functions	Maximum Polynomial Order	Maximum Interaction Order
10	1	0	0
20	9	2	2
30	13	3	2
40	18	3	2
50	23	3	2
60	21	4	2
70	23	5	2
80	30	5	2
90	29	5	3
100	32	5	2

TABLE III

NUMBER OF BASIS FUNCTIONS, MAXIMUM POLYNOMIAL ORDER, AND MAXIMUM INTERACTION ORDER SELECTED UNDER DIFFERENT SAMPLE SIZES (HJORRINGVEJ). POLYNOMIAL ORDER AND INTERACTION ORDER OF 0 INDICATES THAT ONLY THE CONSTANT TERM IS SELECTED.

Number of Samples	Number of Basis Functions	Maximum Polynomial Order	Maximum Interaction Order
10	1	0	0
20	9	2	2
30	14	4	2
40	19	3	2
50	22	4	2
60	23	4	2
70	26	3	2
80	27	4	3
90	31	5	3
100	32	5	3

loss and the reliability interval (defined by the 5% and 95% quantiles) along the propagation range for the two terrains, estimated by the proposed APCE and MC reference. For both Jerslev and Hjørringvej, the APCE mean curve overlaps the MC reference perfectly over the entire distance, including regions with pronounced local fading-like fluctuations. The reliability interval is also accurately reproduced. In Fig. 5, the 5-th and 95-th percentiles estimated by the APCE closely follow the edges of the MC reliability interval, indicating that the proposed surrogate captures not only the expected path loss but also the spread of path loss with high-fidelity.

To further compare the proposed approach against other PCE methods, standard PCE described in Appendix A and the sparse PCE constructed using the LARS algorithm shown in Appendix B), Table IV reports the minimum and maximum relative errors over thirty independent training sets for the mean, 5th, and 95th percentiles. All methods use the same training sets ($N_s = 30$). For the mean path loss, all PCE methods achieve sub-percent accuracy, suggesting that the average trend can be captured with limited samples. Nonetheless, APCE consistently yields the smallest error range, with

the most notable improvement on Hjørringvej, where the maximum mean error decreases from 0.52% (standard PCE) and 0.68% (sparse PCE) to 0.27%. The advantage of APCE becomes more pronounced for the reliability interval: for Jerslev, the worst-case error decreases to 0.75% for both the 5th percentile (from 1.15% and 1.00%) and the 95th percentile (from 2.04% and 1.80%). For Hjørringvej, APCE reduces the maximum error on the 5th percentile from 2.53% and 3.30% to 0.77%, and on the 95th percentile from 2.50% and 4.29% to 0.67%. These results demonstrate that APCE is particularly effective in capturing uncertainty bounds under a limited training budget.

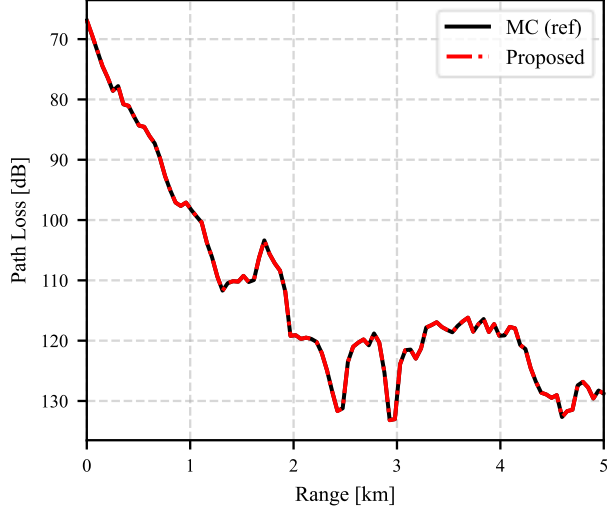
To further assess the robustness of the proposed method with respect to the training samples, we investigate how the relative error ((13)-(15)) evolves as the number of training samples increases. Specifically, we consider $N_s \in \{30, 60, 100, 150, 200, 250, 300\}$. For each N_s , thirty independent training sets are generated and used to construct the corresponding surrogate models. The relative errors of the estimated mean, 5th percentile, and 95th percentile of the path loss are then computed with respect to the MC reference. Fig. 6 summarizes the results, where the solid lines show the average (over the 30 trials) of the relative error and the shaded bands indicate the minimum–maximum of errors across the trials.

As shown in Fig. 6(a)–(b), all methods yield small mean errors, and the average error generally decreases as N_s increases. For Jerslev, the Standard PCE error also exhibits a clear downward trend with increasing N_s , reaching a comparable level to the proposed APCE at large sample sizes. Across most of the sampling range, APCE achieves the lowest or near-lowest average mean error, while maintaining consistently narrow error bands, indicating strong robustness to the choice of training sets. In contrast, the sparse PCE is noticeably less stable for small N_s (e.g., around $N_s = 60$), where both the average error and the spread increase markedly, suggesting a higher sensitivity to the particular training realization in the undersampled regime.

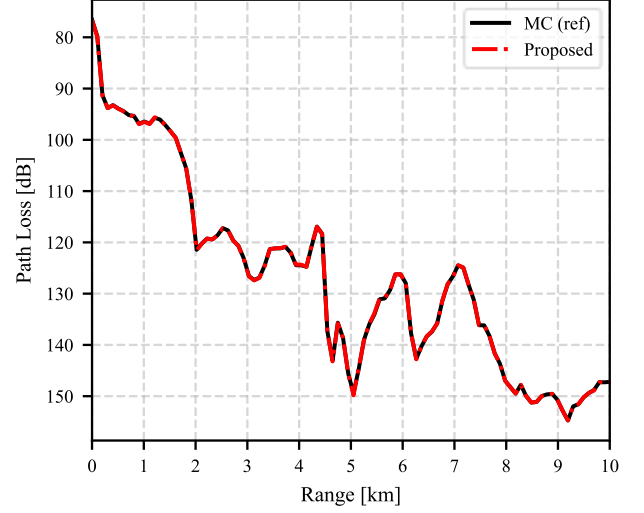
The differences become more pronounced for the quantile estimation that defines the reliability interval. In Fig. 6(c)–(f), APCE maintains low average errors for both the 5th and 95th percentiles and shows a markedly narrower error range, demonstrating improved robustness to the training-set selection. By comparison, the sparse PCE again exhibits large variability at small N_s , with occasional error spikes and wide bands, while the standard PCE tends to level off at a higher error floor and does not consistently reduce its error spread as N_s grows.

V. CONCLUSION

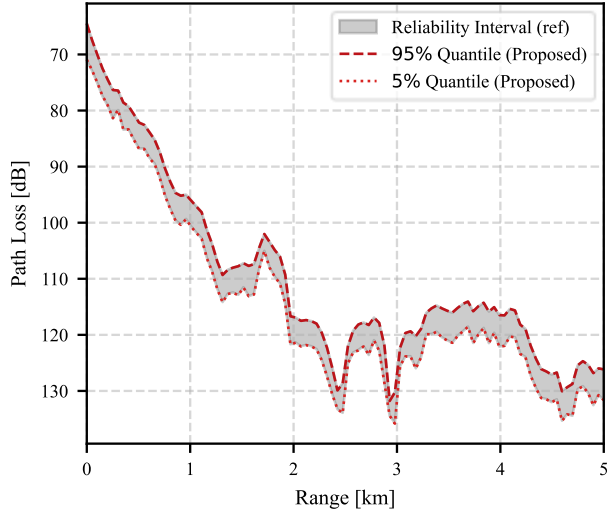
This paper has presented an efficient uncertainty quantification method for radio wave propagation over irregular terrains by combining the two-way parabolic wave equation method with an adaptive polynomial chaos expansion (APCE). The proposed APCE automatically selects and enriches the polynomial basis on the basis of variance contributions and LOOCV error, thereby constructing compact and accurate surrogate models without the need to predefine the polynomial order or rely on strong sparsity assumptions.



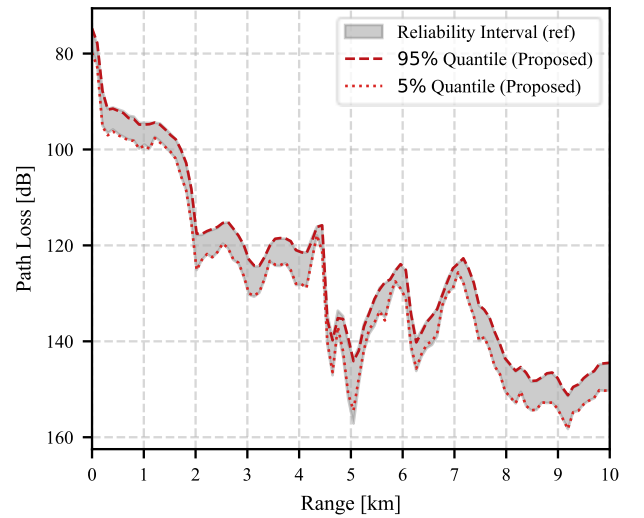
(a) Mean (Jerslev)



(b) Mean (Hjorringvej)



(c) Reliability Interval (Jerslev)

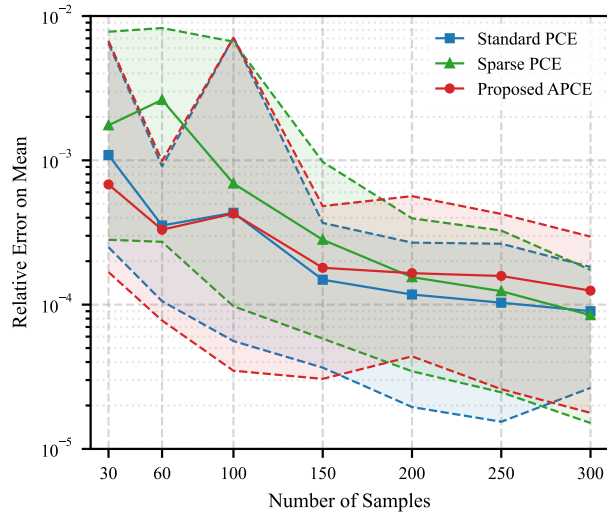


(d) Reliability Interval (Hjorringvej)

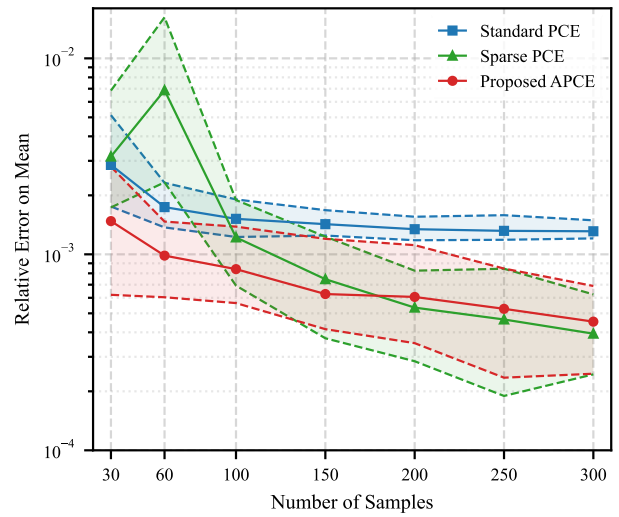
Fig. 5. Mean and reliability interval (5%–95% quantiles) of the path loss versus range for the Jerslev and Hjorringvej terrain profiles. The proposed APCE method with 30 PWE simulations is validated against the Monte Carlo (MC) reference using 10^5 simulations.

TABLE IV
MINIMUM AND MAXIMUM RELATIVE ERRORS OF THE MEAN (13) AND THE 5TH/95TH PERCENTILES (14)–(15) OF THE PATH LOSS OVER 30 INDEPENDENT TRAINING SETS ($N_s = 30$).

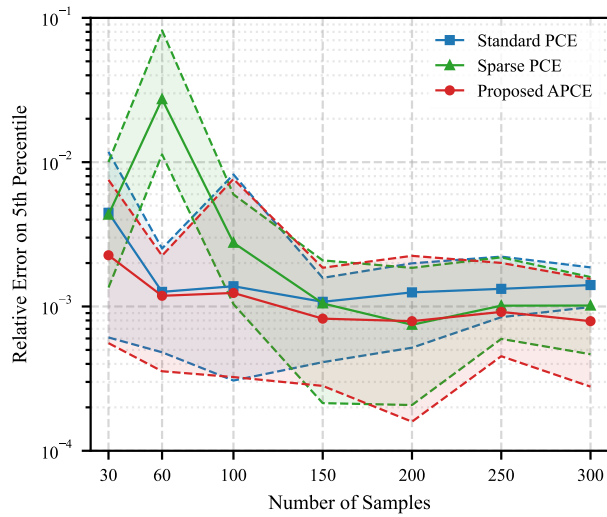
Terrain	Method	Error on Mean		Error on 5th Percentile		Error on 95th Percentile	
		Min.	Max.	Min.	Max.	Min.	Max.
Jerslev	Standard PCE	0.02%	0.64%	0.06%	1.15%	0.13%	2.04%
	Sparse PCE	0.02%	0.77%	0.13%	1.00%	0.24%	1.80%
	Proposed APCE	0.01%	0.67%	0.05%	0.75%	0.04%	0.75%
Hjorringvej	Standard PCE	0.17%	0.52%	0.36%	2.53%	0.46%	2.50%
	Sparse PCE	0.17%	0.68%	0.44%	3.30%	0.68%	4.29%
	Proposed APCE	0.06%	0.27%	0.34%	0.77%	0.26%	0.67%



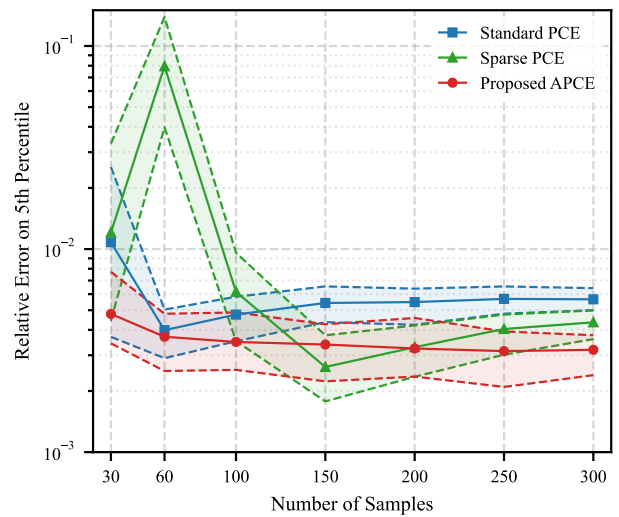
(a) Error on mean (Jerslev)



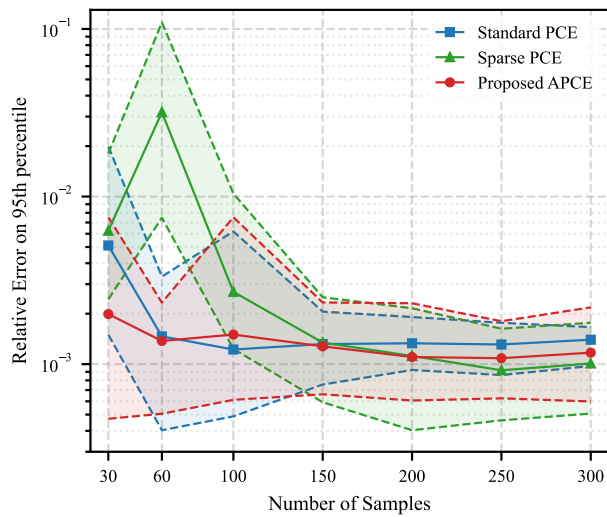
(b) Error on mean (Hjorringvej)



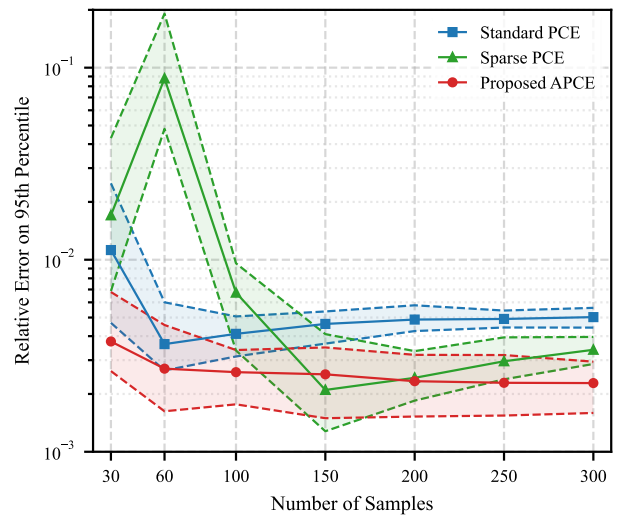
(c) Error on 5th percentile (Jerslev)



(d) Error on 5th percentile (Hjorringvej)



(e) Error on 95th percentile (Jerslev)



(f) Error on 95th percentile (Hjorringvej)

Fig. 6. Relative error statistics versus the number of training samples for the Jerslev and Hjorringvej terrain profiles. Solid lines show the mean relative errors (over 30 independent training sets), and shaded bands (bounded by dashed lines) indicate the minimum–maximum error band across the trials. Results are shown for the mean (a)–(b), the 5th percentile (c)–(d), and the 95th percentile (e)–(f), comparing the Standard PCE, sparse PCE, and the proposed APCE.

Two realistic terrain profiles, Jerslev and Hjorringvej, have been investigated. For both cases, the proposed APCE provides mean, 5% quantile, and 95% quantile of the path loss that closely match MC reference results, while requiring only a small number of PWE simulations. Compared with the standard PCE of fixed total order and with the sparse PCE constructed via LARS, the adaptive method achieves significantly smaller errors, especially for the reliability interval, and exhibits much more stable behavior across different sampling numbers and independent realizations.

Future work may extend the proposed method to a wider range of propagation environments, where terrain-induced variability may exhibit different statistical behaviors. Furthermore, considering the advantage of the proposed method, we should apply it to other computational electromagnetic problems as well.

APPENDIX A

STANDARD POLYNOMIAL CHAOS EXPANSION

Standard PCE refer to as a PCE constructed using a polynomial basis set \mathcal{A} , which is truncated using the maximum total-order criterion with order O_T . The expansion coefficients are estimated via ordinary least-squares regression (10). The corresponding multi-indices set is:

$$\Lambda_{O_{Tmax}}^{N_d} = \{\boldsymbol{\alpha} \in \mathbb{N}^{N_d} : \sum_{i=1}^{N_d} \alpha_i \leq O_{Tmax}\} \quad (16)$$

whose cardinality is

$$\text{card}(\Lambda_{O_T}^{N_d}) = \binom{N_d + O_T}{N_d} = \frac{(N_d + O_T)!}{N_d! O_T!}. \quad (17)$$

where N_d denotes the number of uncertain input parameters. For the five-dimensional problem considered in this paper ($N_d = 5$), the resulting number of polynomial basis functions for different choices of the maximum total order is summarized in Table A-I.

TABLE A-I
NUMBER OF POLYNOMIAL BASIS FUNCTIONS FOR STANDARD PCE
($N_d = 5$)

Maximum Total Order	1	2	3	4	5	6	7
Number of Polynomials	6	21	56	126	252	462	792

APPENDIX B

SPARSE POLYNOMIAL CHAOS EXPANSION

To promote sparsity in the PCE representation and enable the estimation of the expansion coefficients from a limited number of samples, an ℓ_1 -regularized regression formulation is adopted:

$$\hat{\mathbf{u}} = \arg \min_{\mathbf{u}} \|\Psi \mathbf{u} - \mathbf{q}\|_2^2 + \lambda \|\mathbf{u}\|_1, \quad (18)$$

which leads to the so-called sparse PCE [16]. The optimization problem (18) can be solved by various sparse-regression algorithms, such as least angle regression (LARS) [17].

APPENDIX C POSTPROCESSING

Once the PCE model is constructed, the mean of the QoI can be calculated analytically from the PCE coefficients as

$$\mathbb{E}(q) = u_{\boldsymbol{\alpha}_0} \quad (19)$$

where $\boldsymbol{\alpha}_0 = [0, 0, \dots, 0]$. Percentile estimates cannot be obtained in closed form from the coefficients alone. Instead, they are efficiently computed by sampling the PCE model using a Monte Carlo procedure. Since the evaluation of polynomial expansions is computationally inexpensive, generating on the order of 10^5 (or more) surrogate-based samples is readily feasible.

ACKNOWLEDGMENT

All the PCE models are constructed with the help of pygpc [35]. The sparse coefficients are determined using the LARS-Lasso solver from scipy [36].

REFERENCES

- [1] A. Yagbasan, C. A. Tunc, V. B. Erturk, A. Altinatas, and R. Mitra, "Characteristic basis function method for solving electromagnetic scattering problems over rough terrain profiles," *IEEE Trans. Antennas Propag.*, vol. 58, no. 5, pp. 1579–1589, May 2010.
- [2] S. Huang, H. Qin, W. Hou, X. Zhang, and X. Zhang, "A generalizable physics-guided convolutional neural network for irregular terrain propagation," *IEEE Trans. Antennas Propag.*, vol. 73, no. 6, pp. 3975–3985, Jun. 2025.
- [3] Q. Guo and Y. L. Long, "Pade second-order parabolic equation modeling for propagation over irregular terrain," *IEEE Antennas Wireless Propag. Lett.*, vol. 16, pp. 2853–2855, 2017.
- [4] C. G. Batista and C. G. do Rego, "A high-order unconditionally stable FDTD-based propagation method," *IEEE Antennas Wireless Propag. Lett.*, vol. 12, pp. 809–812, 2013.
- [5] E. O. Nuallain, "An efficient integral equation-based electromagnetic propagation model for terrain," *IEEE Trans. Antennas Propag.*, vol. 53, no. 5, pp. 1836–1841, May 2005.
- [6] M. A. N. Silva, E. Costa, and M. Liniger, "Analysis of the effects of irregular terrain on radio wave propagation based on a three-dimensional parabolic equation," *IEEE Trans. Antennas Propag.*, vol. 60, no. 4, pp. 2138–2143, 2012.
- [7] H. Qin, S. An, and X. Zhang, "Efficient two-way parabolic equation method with sparse Fourier transform for radio wave propagation over irregular terrain," in *Proceedings of the Photonics & Electromagnetics Research Symposium (PIERS)*, Chengdu, China, 2024, pp. 1–7.
- [8] Q. Guo and Y. Long, "Two-way parabolic equation method for radio propagation over rough sea surface," *IEEE Trans. Antennas Propag.*, vol. 68, no. 6, pp. 4839–4847, Jun. 2020.
- [9] H. Qin and X. Zhang, "Efficient radio wave propagation modeling in tunnels with a sparse Fourier transform-based split-step parabolic equation method," *IEEE Antennas Wireless Propag. Lett.*, vol. 22, no. 10, pp. 2442–2446, Oct. 2023.
- [10] IEEE Standards Association, *IEEE Recommended Practice for Antenna Measurements*, IEEE Standard 149-2021, pp. 1–207, Feb. 2022.
- [11] International Telecommunication Union, Radiocommunication Sector (ITU-R), "Reference radiation patterns of omnidirectional, sectoral and other antennas for the fixed and mobile services for use in sharing studies in the frequency range from 400 MHz to about 70 GHz," Recommendation ITU-R F.1336-5, Geneva, Switzerland, Jan. 2019.
- [12] X. Zhu, L. Di Rienzo, X. Ma, and L. Codecasa, "Enhanced Multilevel Monte Carlo Method Applied to FDTD for Probability Distribution Estimation," *IEEE Trans. Antennas Propag.*, vol. 71, no.10, pp.8390-8395, Oct. 2023.
- [13] S. An, H. Qin, and X. Zhang, "Efficient uncertainty quantification with subspace pursuit for FDTD-based microwave circuit models," in *Proceedings of the Photonics & Electromagnetics Research Symposium (PIERS)*, Chengdu, China, 2024, pp. 1–5.

- [14] O. L. Maitre and O. M. Knio, *Spectral Methods for Uncertainty Quantification: With Applications to Computational Fluid Dynamics*, Springer Netherlands, 2012.
- [15] D. Xiu, *Numerical Methods for Stochastic Computations: A Spectral Method Approach*, Princeton, NJ, USA: Princeton University Press, 2010.
- [16] N. Lüthen, S. Marelli, and B. Sudret, “Sparse polynomial chaos expansions: Literature survey and benchmark,” *SIAM/ASA J. Uncertain. Quantif.*, vol. 9, no. 2, pp. 593–649, 2021.
- [17] G. Blatman and B. Sudret, “Adaptive sparse polynomial chaos expansion based on least angle regression,” *J. Comput. Phys.*, vol. 230, no. 6, pp. 2345–2367, 2011.
- [18] N. Lüthen, S. Marelli, and B. Sudret, “Automatic selection of basis-adaptive sparse polynomial chaos expansions for engineering applications,” *Int. J. Uncertain. Quantif.*, vol. 12, no. 3, 2022.
- [19] D. Hao, J. Zhang, X. Yue, and L. Chen, “Combined dimensionality reduction based adaptive polynomial chaos expansion for high-dimensional reliability analysis,” *Reliab. Eng. Syst. Saf.*, no. 111324, 2025.
- [20] J. D. Jakeman, M. S. Eldred, and K. Sargsyan, “Enhancing l_1 -minimization estimates of polynomial chaos expansions using basis selection,” *J. Comput. Phys.*, vol. 289, pp. 18–34, 2015.
- [21] S. An, L. Di Rienzo, H. Qin, X. Zhu, X. Zhang, and L. Codecasa, “Multilevel Monte Carlo coupled with the parabolic wave equation method for uncertainty analysis of radio wave propagation in tunnels,” *IEEE Trans. Antennas Propag.*, pp. 1–1, 2025.
- [22] X. Zhang, N. Sood, J. K. Siu, and C. D. Sarris, “Statistical modeling of electromagnetic wave propagation in tunnels with rough walls using the vector parabolic equation method,” *IEEE Trans. Antennas Propag.*, vol. 67, no. 4, pp. 2645–2654, 2019.
- [23] G. B. Saturnino, A. Thielscher, K. H. Madsen, T. R. Knösche, and K. Weise, “A principled approach to conductivity uncertainty analysis in electric field calculations,” *Neuroimage*, vol. 188, pp. 821–834, 2019.
- [24] T. Gerstner and M. Griebel, “Dimension-adaptive tensor-product quadrature,” *Computing*, vol. 71, no. 1, pp. 65–87, 2003.
- [25] M. Levy, *Parabolic Equation Methods for Electromagnetic Wave Propagation*, London, U.K.: IEE, 2000.
- [26] G. Blatman and B. Sudret, “Sparse polynomial chaos expansions and adaptive stochastic finite elements using a regression approach,” *C. R. Méc.*, vol. 336, no. 6, pp. 518–523, 2008.
- [27] D. Xiu and G. E. Karniadakis, “The Wiener–Askey polynomial chaos for stochastic differential equations,” *SIAM J. Sci. Comput.*, vol. 24, no. 2, pp. 619–644, 2002.
- [28] J. C. Helton and F. J. Davis, “Latin hypercube sampling and the propagation of uncertainty in analyses of complex systems,” *Reliab. Eng. Syst. Saf.*, vol. 81, no. 1, pp. 23–69, 2003.
- [29] D. Loukrezis, E. Diehl, and H. De Gerssem, “Multivariate sensitivity-adaptive polynomial chaos expansion for high-dimensional surrogate modeling and uncertainty quantification,” *Appl. Math. Model.*, vol. 137, 2025, Art. no. 115746.
- [30] J. Hampton and A. Doostan, “Basis adaptive sample efficient polynomial chaos (BASE-PC),” *J. Comput. Phys.*, vol. 371, pp. 20–49, 2018.
- [31] L. Wegert, L. Di Rienzo, L. Codecasa, S. An, M. Ziolkowski, A. Hunold, I. Lange, T. Kalla, and J. Haueisen, “The influence of tissue conductivity uncertainty on the nerve activation thresholds in non-invasive electrical phrenic nerve stimulation,” *Biocybern. Biomed. Eng.*, vol. 45, no. 4, pp. 697–706, 2025.
- [32] J. T. Hviid, J. B. Andersen, J. Toftgard, and J. Bojer, “Terrain-based propagation model for rural area—An integral equation approach,” *IEEE Trans. Antennas Propag.*, vol. 43, no. 1, pp. 41–46, Jan. 1995.
- [33] H. Qin and X. Zhang, “Comparative analysis of finite-difference and split-step based parabolic equation methods for tunnel propagation modelling,” *IET Microw. Antennas Propag.*, vol. 18, no. 2, pp. 59–72, 2024.
- [34] A. K. Gupta and S. Nadarajah, *Handbook of Beta Distribution and Its Applications*, New York, NY, USA: Marcel Dekker, 2004.
- [35] K. Weise, L. Poßner, E. Müller, R. Gast, and T. R. Knösche, “Pygpc: A sensitivity and uncertainty analysis toolbox for Python,” *SoftwareX*, vol. 11, 2020.
- [36] P. Virtanen, R. Gommers, T. E. Oliphant, M. Haberland, T. Reddy, D. Cournapeau, *et al.*, “SciPy 1.0: Fundamental algorithms for scientific computing in Python,” *Nat. Methods*, vol. 17, pp. 261–272, 2020.